ACS Catalysis

Letter

pubs.acs.org/acscatalysis

Vanadium-Node-Functionalized UiO-66: A Thermally Stable MOF-Supported Catalyst for the Gas-Phase Oxidative Dehydrogenation of Cyclohexene

Huong Giang T. Nguyen,[†] Neil M. Schweitzer,[†,§] Chih-Yi Chang,[†] Tasha L. Drake,[†] Monica C. So,[†] Peter C. Stair,[†] Omar K. Farha,*[,†,‡] Joseph T. Hupp,*[,†] and SonBinh T. Nguyen*[,†]

[†]Department of Chemistry and the Institute of Catalysis for Energy Processes, Northwestern University, 2145 Sheridan Road, Evanston, Illinois 60208, United States

[§]Center for Catalysis and Surface Science, Northwestern University, 2137 Tech Drive, Evanston, Illinois 60208, United States

[‡]Department of Chemistry, Faculty of Science, King Abdulaziz University, Jeddah, Saudi Arabia

Supporting Information

ABSTRACT: The OH groups on the Zr-based nodes of ultrastable UiO-66 can be metallated with V^V ions in a facile fashion to give the derivative VUiO-66. This metallated MOF exhibits high stability over a broad temperature range and displays high selectivity for benzene under low-conversion conditions in the vapor-phase oxidative dehydrogenation of cyclohexene (activation energy ~110 kJ/mol). The integrity of the MOF is maintained after catalysis as determined by PXRD, ICP-AES, and SEM.

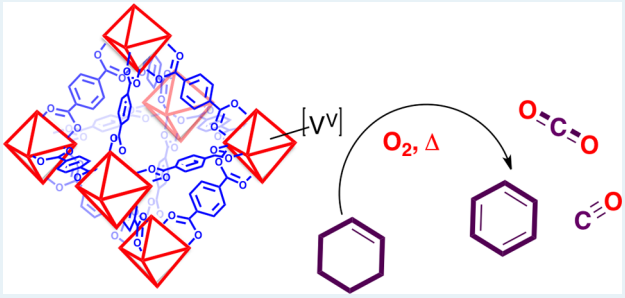

KEYWORDS: *metal−organic framework, gas-phase catalysis, cyclohexene oxidation, UiO-66, vanadium*

Although metal−organic frameworks (MOFs),[1−3] a crystalline and porous class of materials, have been extensively used as catalysts or catalyst supports[4−11] in solution phase, their usage in gas- and vapor-phase catalysis has been rare[12−24] and limited thus far, with the majority of reported examples focused on the oxidation of CO to CO_2. Nonetheless, MOFs possess many desirable properties that make them highly attractive as gas-phase catalysts: (1) Their intrinsic crystallinity allows for the design and deployment of single-site, and uniformly dispersed catalytic species, yielding catalysts with excellent selectivity. (2) Their high surface areas—in comparison with zeolites, metal oxide supports, and other porous materials—can engender a very high density of catalytic sites, enabling higher chances of contact with substrates. (3) Their tailorable porosity can provide a special cavity environment for substrates to interact with catalytically active sites, similar conceptually to the secondary interaction spheres of enzyme active sites, which can further enhance activity and selectivity.

For a MOF to be broadly used as a catalyst for gas-phase reactions, it must have high thermal stability, good structural stability to activation, and excellent mechanical robustness. Given the high temperatures (>200 °C) that are typically required for gas-phase catalysis, the relatively low thermal stability of many early MOFs was often thought as a major obstacle to their realization as viable heterogeneous catalysts in industrially valuable processes. Although there were relatively few MOFs capable of withstanding such high temperatures for prolonged periods without physical or chemical degradation,[25] recent synthetic progresses have yielded many frameworks that are remarkably stable to high temperatures. Such enhanced thermal stability of the frameworks, and therefore of the catalytically active species that they support, are critical for the exploration of MOFs as heterogeneous catalysts and catalyst supports. Herein, we report the functionalization of the hydroxyl-presenting nodes of UiO-66 with V^V ions, which constitutes a highly stable MOF-supported catalyst for the gas-phase oxidation of cyclohexene. This metallated MOF exhibits high stability over a broad temperature range and shows high catalytic selectivity for benzene formation under low-conversion conditions. Our work illustrates that MOF platforms with high thermal stability can, indeed, be used as catalysts and catalyst supports for high-temperature gas-phase chemical transformations.

As the ideal MOF support platform, we selected the Zr-based UiO-66 framework,[26] a MOF known to have exceptional thermal and mechanical stability. UiO-66 is composed of 12-coordinate $Zr(O)_4(OH)_4$ nodes, each linked to 12 carboxylates of terephthalate ligands to form super tetrahedral and super octahedral cages (Scheme 1) with apertures of approximately 6 Å. It has been reported to be stable to up to ~540 °C, based on thermogravimetric analysis, and up to ~375 °C, based on

Received: February 4, 2014
Revised: May 30, 2014
Published: June 2, 2014

   dx.doi.org/10.1021/cs5001448 | ACS Catal. 2014, 4, 2496−2500

Scheme 1. Metallation of UiO-66 with O═V(acac)$_2$[a]

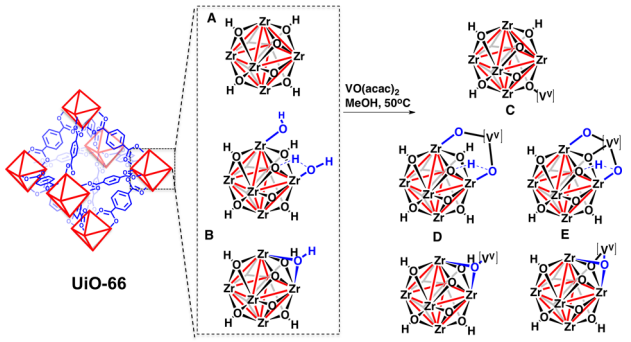

[a]Left: Structure of UiO-66 and its proposed idealized (**A**) and defective (**B**) hydroxyl-presenting nodes. Right: Proposed possible products **C**−**E**. [b]For presentation clarity, the central clusters in structures **A**−**E** are drawn without charge-compensating ligands.

temperature-programmed PXRD.[27] It is also stable to water and many organic solvents.[26] Additionally, it can withstand high pressure without mechanical degradation,[28] making it highly attractive as a support in fixed-bed flow reactors for gas-phase reactions.[29]

As a model reaction for testing UiO-66-based catalysts, we selected the gas-phase oxidative dehydrogenation of cyclohexene into benzene (eq 1). This transformation is of potential

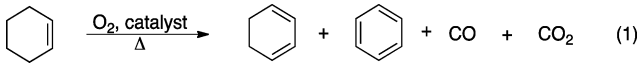

(1)

interest in benzene purification because cyclohexene is a persistent impurity in large-scale benzene production (~20 M tons/yr globally).[30] The possibility for this reaction to yield several different products in the presence of oxygen additionally serves as a convenient probe for catalyst activity/selectivity evaluation. We note that although cyclohexene is typically a liquid at ambient temperature and pressure, the vapor-phase oxidative dehydrogenation of cyclohexene has been reported.[30−32] Given that the Zr^{IV} ions in the node of UiO-66 have minimal activity in oxidation catalysis,[33] we chose to incorporate redox-active V^V ions via reaction with the available −OH groups of the nodes. We note that Laribi et al. have demonstrated that the −OH groups on the Zr node of UiO-67, an analogue of UiO-66, can react with and immobilize Mg^{II} ions as well as Au^I phosphine species.[34] More recently, the −OH groups on the node of the Zr-based clusters in the NU-1000 MOF platform have also been metallated with Zn^{II} and Al^{III} using atomic layer deposition.[35]

By metallating the −OH groups on the nodes of UiO-66 with V^V ions, we were encouraged by previous reports of supported vanadium oxides being capable of catalyzing the oxidative dehydrogenation of propane,[36−38] *n*-butane,[39−41] and cyclohexane.[42] We envisioned the node of UiO-66 to behave as a discrete solid-support-like "ligand" for the V^V center, but with a more well-defined display of OH groups that affords only one type of catalytic species (Scheme 1, structures **A** and **C**), as opposed to the many species that may be present in conventional vanadium oxide-supported heterogeneous catalysts.[43] However, we note that UiO-66 has been reported to have missing linkers, possibly exposing additional −OH groups[44] that could participate in metal-binding (Scheme 1, structure **B**). Although there have been examples of MOF-based gas-phase catalysis with active sites present at the node,[15,20−22] on ligands,[12,13] or being encapsulated in the MOF pores[16,17] (including a recent report on the use of Au nanoparticle@UiO-66 for CO oxidation[24]), our work represents one of a very few examples of a node-supported active metal species.

Microcrystalline samples of UiO-66, a white powder comprising octahedral particles of ~0.5−1 μm, was synthesized using a slight modification of a reported procedure that employs acetic acid as a modulator.[45] Its PXRD pattern agreed well with the simulated pattern, and its BET surface area (~1240 ± 120 m^2/g) matched the reported values (Figures S1−S3 in the Supporting Information (SI)). TGA (Figure S4 in the SI) and micropore volume (0.47 cm^3/g) analyses of the MOF suggested ~0.6/12 of the 1,4-benzene dicarboxylate (BDC) linkers are missing.[46] (This is the equivalence of 5% of the sites that can be occupied by the ditopic linkers or ~9.5% of the sites that can be occupied by a monotopic modulator/ligand). The NMR spectrum in DMSO-d_6 (Figure S14 in the SI) of D_2SO_4-dissolved UiO-66 after activation showed a small amount of acetic acid (~11.5 mol % of the total ligands), which presumably existed as acetate ions that cap the missing-linker sites after synthesis (see Figure S10 in the SI for supporting data).

The metallation of UiO-66 with vanadyl acetylacetonate (~8 Å in size) was carried out in MeOH to afford VUiO-66 as an off-yellow powder with unchanged PXRD pattern and nearly unchanged BET surface area (1220 ± 100 m^2/g, 0.46 cm^3/g micropore volume) (Figures S1−S3 in the SI). Inductively coupled plasma atomic-emission analysis (ICP−AES) indicated a V loading of ~0.10 ± 0.01 V/Zr. NMR analysis of the D_2SO_4-dissolved metallated MOF indicated that very little of the initially present acetic acid (acetate) remained and that the acac ligand was not present (Figures S14−S15 in the SI). Thus, we speculate that the V reagent has reacted with the −OH groups (shown in blue, Scheme 1, structure **B**) that were present *at the missing-linker sites of the nodes*. Presumably, these reactive and more-accessible groups could arise if the acetate caps in the as-synthesized materials were displaced by water during the metallation process (see Scheme 1, structures **B** and **D** for some possible binding modes and Figure S10 in the SI for supporting data). Indeed, when we attempted to remove the acetate capping by treating the as-synthesized UiO-66 with a DMF solution of diluted HCl, we observed the growth of additional peaks in its in situ DRIFTS spectrum that can be attributed to new −OH species (Figure S10 in the SI). In combination with the NMR analysis, these data strongly supported the hypothesis that the −OH groups at missing-linker sites could form and react with the O═V(acac)$_2$ reagent.

Although we cannot rule out the possibility that the bridging hydroxyl groups on the nodes of UiO-66 also reacted with O═V(acac)$_2$, we suspect that the low reactivity of these groups[34] made them less likely to react before the −OH groups at missing-linker sites. In addition, the low density of metallation (a maximum 15% of bridging hydroxyl groups being metallated if there were no missing-linker sites) made it difficult to quantify, using DRIFTS,[34] the amount of bridging −OH groups that could compete for the available O═V(acac)$_2$. Indeed, the DRIFTS spectra (Figure S9 in the SI) of activated samples of UiO-66, VUiO-66, and UiO-66 that have been capped with either acetate or benzoate (see Sections S2−S3 in the SI) all showed similarly sharp hydroxyl peaks ~3674 cm^{-1}, attributable to the bridging −OH group on the node.[34,47]

dx.doi.org/10.1021/cs5001448 | ACS Catal. 2014, 4, 2496−2500

The XPS spectrum of VUiO-66 showed a V 2p peak with binding energy of 517 eV, consistent with the value expected for V^V (Figure S11 in the SI). The visible-Raman spectrum of an as-prepared VUiO-66 sample does not show the signature band at 993 cm^{-1} for the V═O moiety in V_2O_5 (Figure S12 in the SI); neither does it show any band that can be attributed to a V═O species, presumably due to a combination of low V loading and the presence of adsorbed water.[48] Heating this sample to 400 °C also did not result in any V═O bands in the 900−1050 cm^{-1} region. Although the UV-Raman spectrum of a VUiO-66 sample that has been heated to 400 °C showed the presence of V−O−Zr bond[48,49] as a broad hump at 700−1018 cm^{-1} (Figure S12 in the SI), we were unable to get better-resolved spectra under the limited laser power and dehydrating conditions of our experiments, for which measurements can be carried out without completely destroying the MOF platform. However, analysis of the diffuse-reflectance UV−vis spectrum of VUiO-66 (Figure S13 in the SI) clearly revealed an edge energy of 3.38 eV that is consistent with the presence of mostly monomeric VO_x species with a minor oligomeric component.[50] Together, these results agreed well with the presence of isolated V^V species expected from the immobilization of monomeric O═V(acac)$_2$ reagent onto −OH sites on the node of UiO-66.

Using O_2 as the oxidant, the oxidative dehydrogenation of cyclohexene was carried out in a packed-bed flow reactor in the 250−350 °C range. At 250 °C and low-conversion conditions (<2% conversion), VUiO-66 catalyzed the formation of benzene with 100% molar selectivity (Figure 1). However,

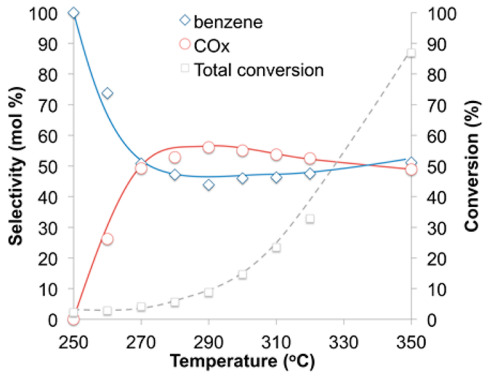

Figure 1. Selectivities (in mol %) for benzene (blue diamonds) and CO_x (CO + CO_2, red circles), and total conversion (%) as a function of temperature. The lines are provided only as visual guides. For individual plots of CO and CO_2 selectivities, please see Figure S18 in the SI.

this molar selectivity quickly degraded (to ∼83 C% when corrected for the C stoichiometry; see Figure S19 in the SI) at slightly higher temperatures. Interestingly, this drop in selectivity leveled out above 270 °C with the majority of the byproducts (∼40−50 mol % CO and CO_2, Figure 1; 17 C%) attributable to combustion; only a very small amount (≪1 mol %, not shown) of cyclohexadiene, the incomplete dehydrogenation product, was observed. A control study of the oxidative dehydrogenation of cyclohexene using the unmetallated parent UiO-66 material showed only minor background reaction (<10% conversion at 350 °C, Figure S20 in the SI), implying that the majority of the catalytic activity was from the supported vanadium species.

The oxidative dehydrogenation of cyclohexene on VUiO-66 exhibits Arrhenius-like behavior in the 260−300 °C temperature range, giving higher conversions at higher temperatures (Figure 2). In the presence of VUiO-66, the oxidative

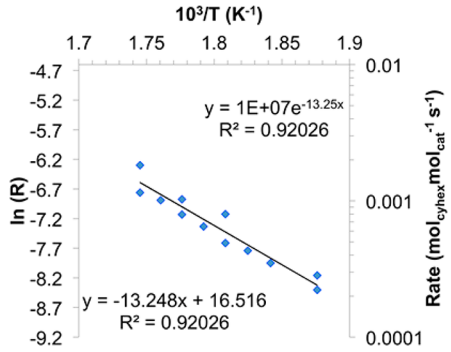

Figure 2. Arrhenius plot for VUiO-66-catalyzed oxidation dehydrogenation of cyclohexene in the differential conversion regime (∼10%) and reaction-rate-limited temperature regime of 260−300 °C where mass-transfer limitations are absent. For consistency, turnover frequency (rate = R) is calculated on the basis of the data obtained at t = 18 h.[53]

dehydrogenation of cyclohexene is calculated to have an activation energy of 110 ± 10 kJ/mol (26.3 kcal/mol), which is comparable to reported values (16−24 kcal/mol) determined by Rioux et al. for various sizes of Pt nanoparticles supported on SBA-15.[32,51] For comparison, VUiO-66 offers much better selectivity for benzene than the best (∼8%) of a series of Co clusters supported on metal oxides[31] and similar selectivity to VO_x on monolithic alumina.[42] However, it is less selective for benzene at high conversions compared with a recently reported Au−Pd/TiO_2 catalyst (99% selectivity at 100% conversion).[30]

The PXRD patterns of the VUiO-66 catalyst after 18 h catalytic runs at several temperatures (Figure 3, left panel) are

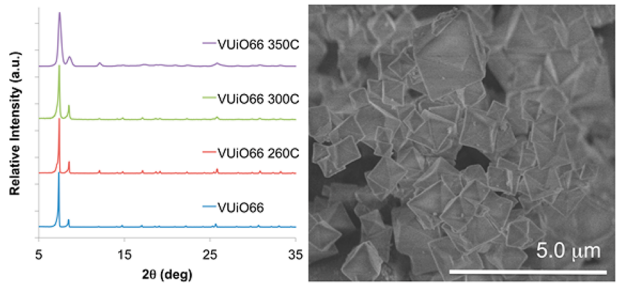

Figure 3. Left: PXRD patterns of UiO-66 and VUiO-66 after catalysis at 260, 300, and 350 °C. Right: SEM image of VUiO-66 particles after catalyzing cyclohexene oxidative dehydrogenation at 350 °C for 18 h.

identical to that of the as-synthesized material, indicating that the crystallinity of the V-functionalized MOF is retained even after prolonged heating at 350 °C. Notably, conversions remain at a stable, high level (∼85%), even after 48 h on stream at 350 °C (Figure S24 in the SI).[52] ICP-AES analysis revealed that the V content (∼0.1 V/Zr) remains the same after catalysis, indicating that there is no leaching of the active site. Consistent with all of these observations, the SEM image of VUiO-66 after catalysis at 350 °C also showed well-defined octahedral particles (Figure 3, right panel), further demonstrating the excellent robustness of the UiO-66 platform.

In summary, we have decorated the hydroxyl-presenting nodes of UiO-66 to form a robust VUiO-66 catalyst and demonstrated it to be active in the gas-phase oxidative

dx.doi.org/10.1021/cs5001448 | ACS Catal. 2014, 4, 2496−2500

dehydrogenation of cyclohexene, selectively forming benzene at low conversion (100 mol % selectivity at 2% conversion). This selectivity remains at a good level (~80 mol % of cyclohexene is converted to benzene at moderate to high conversions), suggesting that the environment of the active catalyst remains unchanged across a broad range of temperatures and reaction conditions. Most notable is the observation that the MOF support maintains excellent structural integrity at temperatures as high as 350 °C, as determined by PXRD, ICP-AES analysis, and SEM imaging.

From a broader perspective, we envision the metallation of the nodes of highly stable MOFs to be a general strategy for the deployment of a broad range of other metal-ion-containing catalysts capable of effecting many important gas-phase reactions. We anticipate that UiO-66, and other emerging ultrastable MOFs[35,54−57] in which metal species can be easily incorporated, will open up new research directions and fulfill the potential of MOFs as a versatile and robust class of supports for heterogeneous gas-phase chemical reactions.

■ ASSOCIATED CONTENT

Supporting Information

Materials and methods; synthesis of UiO-66, capped-UiO-66, HCl-treated UiO-66, and VUiO-66; PXRD patterns, N_2 isotherms; TGA, XPS, Raman, DRIFTS, and catalysis data. This material is available free of charge via the Internet at http://pubs.acs.org.

■ AUTHOR INFORMATION

Corresponding Authors

*Phone: +1 847-467-4934. E-mail: o-farha@northwestern.edu.
*Phone: +1 847-491-3501. E-mail: j-hupp@northwestern.edu.
*Phone: +1 847-467-3347. E-mail: stn@northwestern.edu.

Notes

The authors declare no competing financial interest.

■ ACKNOWLEDGMENTS

This work was supported by the Chemical Sciences, Geosciences, and Biosciences Division, U.S. Department of Energy through a grant (DE FG02-03ER15457) to the Institute of Catalysis for Energy Processes (ICEP) at Northwestern University (assistantship for H.G.T.N). The catalysis experiments were carried out at the Clean Catalysis Facility of Northwestern University Center for Catalysis and Surface Science, which acknowledges funding from the Department of Energy (DE-FG02-03ER15457 and DE-AC02-06CH11357) used for the purchase of the Thermo Nicolet/Harrick DRIFTS system and the Altamira AMI-200. M.C.S. acknowledges support from the Department of Defense through the National Defense Science & Engineering Graduate Fellowship (NDSEG) Program. Experimental facilities at the Integrated Molecular Structure Education and Research Center (IMSERC), Keck Biophysics Facility, and the Northwestern University Atomic- and Nanoscale Characterization Experimental Center (EPIC, Keck-II) at Northwestern University were purchased with grants from NSF-NSEC, NSF-MRSEC, the Keck Foundation, the state of Illinois, and Northwestern University. We thank Mr. Kevin Schwartzenberg and Mr. Cornelius Audu for help with TGA analysis and Ms. Stephanie Kwon for helpful discussions regarding the operations of the instruments in the Clean Catalysis Facility. We thank the reviewers of an initial version of this manuscript for helpful discussions that improved it.

■ ABBREVIATIONS

MOF = metal−organic frameworks; BET = Brunauer−Emmett−Teller; TGA = thermogravimetric analysis; PXRD = powder X-ray diffraction; SEM = scanning electron microscopy; TOF-SIMS = time-of-flight secondary ion mass spectrometry

■ REFERENCES

(1) Férey, G. *Chem. Soc. Rev.* **2008**, *37*, 191−214.
(2) Furukawa, H.; Cordova, K. E.; O'Keeffe, M.; Yaghi, O. M. *Science* **2013**, *341*, 1230444/1−12.
(3) Horike, S.; Shimomura, S.; Kitagawa, S. *Nat. Chem.* **2009**, *1*, 695−704.
(4) Corma, A.; Garcia, H.; Llabrés i Xamena, F. X. *Chem. Rev.* **2010**, *110*, 4606−4655.
(5) Dhakshinamoorthy, A.; Alvaro, M.; Garcia, H. *Catal. Sci. Technol.* **2011**, *1*, 856−867.
(6) Dhakshinamoorthy, A.; Alvaro, M.; Garcia, H. *Chem. Commun.* **2012**, *48*, 11275−11288.
(7) Farrusseng, D.; Aguado, S.; Pinel, C. *Angew. Chem., Int. Ed.* **2009**, *48*, 7502−7513.
(8) Lee, J.; Farha, O. K.; Roberts, J.; Scheidt, K. A.; Nguyen, S. T.; Hupp, J. T. *Chem. Soc. Rev.* **2009**, *38*, 1450−1459.
(9) Ma, L.; Abney, C.; Lin, W. *Chem. Soc. Rev.* **2009**, *38*, 1248−1256.
(10) Yoon, M.; Srirambalaji, R.; Kim, K. *Chem. Rev.* **2011**, *112*, 1196−1231.
(11) Gascon, J.; Corma, A.; Kapteijn, F.; Llabrés i Xamena, F. X. *ACS Catal.* **2013**, *4*, 361−378.
(12) Kleist, W.; Maciejewski, M.; Baiker, A. *Thermochim. Acta* **2010**, *499*, 71−78.
(13) Zhang, X.; Llabrés i Xamena, F. X.; Corma, A. *J. Catal.* **2009**, *265*, 155−160.
(14) Kim, J.; Jin, M.; Lee, K.; Cheon, J.; Joo, S.; Kim, J.; Moon, H. *Nanoscale Res. Lett.* **2012**, *7*, 461−468.
(15) Henschel, A.; Gedrich, K.; Kraehnert, R.; Kaskel, S. *Chem. Commun.* **2008**, *44*, 4192−4194.
(16) Hermes, S.; Schröter, M.-K.; Schmid, R.; Khodeir, L.; Muhler, M.; Tissler, A.; Fischer, R. W.; Fischer, R. A. *Angew. Chem., Int. Ed.* **2005**, *44*, 6237−6241.
(17) Jiang, H.-L.; Liu, B.; Akita, T.; Haruta, M.; Sakurai, H.; Xu, Q. *J. Am. Chem. Soc.* **2009**, *131*, 11302−11303.
(18) Liang, D.-D.; Liu, S.-X.; Ma, F.-J.; Wei, F.; Chen, Y.-G. *Adv. Synth. Catal.* **2011**, *353*, 733−742.
(19) Gascon, J.; Hernández-Alonso, M. D.; Almeida, A. R.; van Klink, G. P. M.; Kapteijn, F.; Mul, G. *ChemSusChem* **2008**, *1*, 981−983.
(20) Denysenko, D.; Werner, T.; Grzywa, M.; Puls, A.; Hagen, V.; Eickerling, G.; Jelic, J.; Reuter, K.; Volkmer, D. *Chem. Commun.* **2012**, *48*, 1236−1238.
(21) Zhao, Y.; Padmanabhan, M.; Gong, Q.; Tsumori, N.; Xu, Q.; Li, J. *Chem. Commun.* **2011**, *47*, 6377−6379.
(22) Zou, R.-Q.; Sakurai, H.; Xu, Q. *Angew. Chem., Int. Ed.* **2006**, *45*, 2542−2546.
(23) Zou, R.-Q.; Sakurai, H.; Han, S.; Zhong, R.-Q.; Xu, Q. *J. Am. Chem. Soc.* **2007**, *129*, 8402−8403.
(24) Wu, R.; Qian, X.; Zhou, K.; Liu, H.; Yadian, B.; Wei, J.; Zhu, H.; Huang, Y. *J. Mater. Chem. A* **2013**, *1*, 14294−14299.
(25) Although several examples of MOFs with high thermal stability have been reported—based on transient thermal excursions during thermogravimetric analysis (TGA)—have been reported, their suitability for high-temperature catalysis would require assessement of stability over prolonged periods of time. As such, TGA measurements are probably best viewed as stability-screening experiments rather than definitive experiments.
(26) Cavka, J. H.; Jakobsen, S.; Olsbye, U.; Guillou, N.; Lamberti, C.; Bordiga, S.; Lillerud, K. P. *J. Am. Chem. Soc.* **2008**, *130*, 13850−13851.

(27) Valenzano, L.; Civalleri, B.; Chavan, S.; Bordiga, S.; Nilsen, M. H.; Jakobsen, S.; Lillerud, K. P.; Lamberti, C. *Chem. Mater.* **2011**, *23*, 1700−1718.
(28) Wu, H.; Yildirim, T.; Zhou, W. *J. Phys. Chem. Lett.* **2013**, *4*, 925−930.
(29) In our hand, VUiO-66 could be pressed into pellets with unchanged PXRD pattern using a high-pressure KBr pellet press.
(30) Dummer, N. F.; Bawaked, S.; Hayward, J.; Jenkins, R.; Hutchings, G. J. *Catal. Today* **2010**, *154*, 2−6.
(31) Lee, S.; Vece, M. D.; Lee, B.; Seifert, S.; Winans, R. E.; Vajda, S. *Phys. Chem. Chem. Phys.* **2012**, *14*, 9336−9342.
(32) Rioux, R. M.; Hsu, B. B.; Grass, M. E.; Song, H.; Somorjai, G. A. *Catal. Lett.* **2008**, *126*, 10−19.
(33) They have, however, been found to display good catalytic activity for other reactions, including hydrolysis reactions. See, for example: (a) Vermoortele, F.; Bueken, B.; Le Bars, G.; Van de Voorde, B.; Vandichel, M.; Houthoofd, K.; Vimont, A.; Daturi, M.; Waroquier, M.; Van Speybroeck, V.; Kirschhock, C.; De Vos, D. E. *J. Am. Chem. Soc.* **2013**, *135*, 11465−11468. (b) Katz, M. J.; Mondloch, J. E.; Totten, R. K.; Park, J. K.; Nguyen, S. T.; Farha, O. K.; Hupp, J. T. *Angew. Chem., Int. Ed.* **2014**, *53*, 497−501.
(34) Larabi, C.; Quadrelli, E. A. *Eur. J. Inorg. Chem.* **2012**, *2012*, 3014−3022.
(35) Mondloch, J. E.; Bury, W.; Fairen-Jimenez, D.; Kwon, S.; DeMarco, E. J.; Weston, M. H.; Sarjeant, A. A.; Nguyen, S. T.; Stair, P. C.; Snurr, R. Q.; Farha, O. K.; Hupp, J. T. *J. Am. Chem. Soc.* **2013**, *135*, 10294−10297.
(36) Cheng, L.; Ferguson, G. A.; Zygmunt, S. A.; Curtiss, L. A. *J. Catal.* **2013**, *302*, 31−36.
(37) Rozanska, X.; Fortrie, R.; Sauer, J. *J. Phys. Chem. C* **2007**, *111*, 6041−6050.
(38) Carrero, C. A.; Keturakis, C. J.; Orrego, A.; Schomacker, R.; Wachs, I. E. *Dalton Trans.* **2013**, *42*, 12644−12653.
(39) Jackson, S. D.; Rugmini, S.; Stair, P. C.; Wu, Z. *Chem. Eng. J.* **2006**, *120*, 127−132.
(40) McGregor, J.; Huang, Z.; Shiko, G.; Gladden, L. F.; Stein, R. S.; Duer, M. J.; Wu, Z.; Stair, P. C.; Rugmini, S.; Jackson, S. D. *Catal. Today* **2009**, *142*, 143−151.
(41) Wu, Z.; Stair, P. C. *J. Catal.* **2006**, *237*, 220−229.
(42) Feng, H.; Elam, J. W.; Libera, J. A.; Pellin, M. J.; Stair, P. C. *J. Catal.* **2010**, *269*, 421−431.
(43) Muylaert, I.; Van Der Voort, P. *Phys. Chem. Chem. Phys.* **2009**, *11*, 2862−2832.
(44) (a) Katz, M. J.; Brown, Z. J.; Colon, Y. J.; Siu, P. W.; Scheidt, K. A.; Snurr, R. Q.; Hupp, J. T.; Farha, O. K. *Chem. Commun.* **2013**, *49*, 9449−9451. (b) See also ref 33a and (c) ref 27.
(45) Schaate, A.; Roy, P.; Godt, A.; Lippke, J.; Waltz, F.; Wiebcke, M.; Behrens, P. *Chem.−Eur. J.* **2011**, *17*, 6643−6651.
(46) (a) Wu, H.; Chua, Y. S.; Krungleviciute, V.; Tyagi, M.; Chen, P.; Yildirim, T.; Zhou, W. *J. Am. Chem. Soc.* **2013**, *135*, 10525−10532. (b) See also ref 33a..
(47) Shearer, G.; Forselv, S.; Chavan, S.; Bordiga, S.; Mathisen, K.; Bjørgen, M.; Svelle, S.; Lillerud, K. *Top. Catal.* **2013**, *56*, 770−782.
(48) Wu, Z.; Kim, H.-S.; Stair, P. C.; Rugmini, S.; Jackson, S. D. *J. Phys. Chem. B* **2005**, *109*, 2793−2800.
(49) Magg, N.; Immaraporn, B.; Giorgi, J. B.; Schroeder, T.; Baumer, M.; Dobler, J.; Wu, Z.; Kondratenko, E.; Cherian, M.; Baerns, M.; Stair, P. C.; Sauer, J.; Freund, H.-J. *J. Catal.* **2004**, *226*, 88−100.
(50) Gao, X.; Wachs, I. E. *J. Phys. Chem. B* **2000**, *104*, 1261−1268.
(51) To our knowledge, there are no reported values for the activation energy for the oxidative dehydrogenation of cyclohexene by other heterogeneous (i.e., supported) VO_x catalysts.
(52) At lower temperatures (260−300 °C), there is some initial catalytic deactivation, presumably due to coking.
(53) As the reaction progresses, the MOF suffers from gradual deactivation that is most likely due to coking based on BET SA and TGA analyses (Figures S21−S23 in the SI), given that its structural integrity and metal loading is maintained (see discussion in the main text).
(54) Morris, W.; Volosskiy, B.; Demir, S.; Gándara, F.; McGrier, P. L.; Furukawa, H.; Cascio, D.; Stoddart, J. F.; Yaghi, O. M. *Inorg. Chem.* **2012**, *51*, 6443−6445.
(55) Jiang, H.-L.; Feng, D.; Liu, T.-F.; Li, J.-R.; Zhou, H.-C. *J. Am. Chem. Soc.* **2012**, *134*, 14690−14693.
(56) Chen, Y.; Hoang, T.; Ma, S. *Inorg. Chem.* **2012**, *51*, 12600−12602.
(57) Feng, D.; Chung, W.-C.; Wei, Z.; Gu, Z.-Y.; Jiang, H.-L.; Chen, Y.-P.; Darensbourg, D. J.; Zhou, H.-C. *J. Am. Chem. Soc.* **2013**, *135*, 17105−17110.